DEVELOPMENT OF A LOW–COST SENSOR SYSTEM FOR USE ON GYROCOPTERS

A. Miraliakbari, M. Hahn, J. Engels

Department of Geomatics, Computer Science and Mathematics, University of Applied Sciences Stuttgart
Schellingstraße 24, D-70174 Stuttgart, Germany
(alvand.miraliakbari, michael.hahn, johannes.engels)@hft-stuttgart.de

Commission I, WG I/2

KEY WORDS: Aerial, Infrared, IMU, GPS, Mosaic, Orthoimage, Thermal, Triangulation

ABSTRACT:

Direct georeferencing of airborne imaging sensors with high precision GNSS and inertial technology is an established practice used in numerous aerial survey mapping projects nowadays. Those integrated systems of high quality aerial cameras and orientation sensors have their price which finds its expression in the high price level of aerial survey mapping projects. The development of an alternative for aerial survey mapping is the challenge of this research. It aims at the development of a low-cost sensor system for capturing aerial colour and thermal images of high photogrammetric quality by using a gyrocopter. Fusion of both images produces pan-sharpened thermal images which are easier to interpret visually.
In this paper we describe the experimental setup of our low-cost system and present first results of gyrocopter image flights using a SLR colour camera and a thermal infrared camera. For controlling the blocks of aerial images as well as for navigational support of the gyrocopter pilot, a GPS aided MEMS-based IMU is used. Orthophotos are generated and orthophoto mosaicking is carried out, both with RGB and thermal infrared images. Horizontal deviations in the order of 5 to 10 m from the planned flight track have been observed in our first four test flights. The recorded GPS/IMU sensor data are analyzed to investigate vibrations of the gyrocopter platform. Most prominent are vibration frequencies of about 13Hz which stem from the rotor. Shock mounts will be used in our future development to absorb the influence of the vibrations onto our sensor platform.

1. INTRODUCTION

In-flight control systems with GPS/IMU sensors are state-of-the-art for direct acquisition of the exterior orientation of airborne sensors. If digital aerial camera equipment or laser scanners are used together with high-quality GPS/inertial systems the overall aerial survey mapping system is of an upper price category. Together with the running costs of aircrafts or helicopters this leads to the current price level of the products of aerial surveys like orthophotos and DTMs.
One possibility to reduce costs is to use inexpensive air vehicles and to equip it with inexpensive sensors like SLR cameras and MEMS-based IMUs. The development of a low-cost sensor system for capturing aerial colour and thermal images of high photogrammetric quality by using a gyrocopter is the challenge of this research. Gyrocopters are lightweight aircrafts of great simplicity, high mission readiness and low acquisition and maintenance costs. During the last couple of years this low-cost vehicles have got approval by aviation authorities in US, Europe and many other countries worldwide.
To capture aerial images on a high photogrammetric quality level by using a gyrocopter is the challenge of this research. Compared to airplanes and helicopters the gyrocopter is a cheap aircraft. Flights with the gyrocopter are not more expensive than touring with a car with the consequence that this opens new opportunities for creating low cost services based on aerial survey. In particular developing countries may benefit from such a system, but it offers also excellent prospects to enter the aerial survey market for small and medium sized companies in Europe.

Like a helicopter, the gyrocopter has horizontal rotor blades, but compared to the former, these blades are not activated by a motor, but only driven by the air flow. The propulsion of the vehicle is achieved by a propeller drive. The advantages of the gyrocopter are: 1) its high stability and security (there is no breakaway of the airflow if the velocity goes below a certain limit; even a motor fail does not necessarily let the vehicle crash) 2) low acquisition prize 3) low consumption of fuel and 4) the possibility to use normal fuel as gasoline.

In a first encouraging experiment (Miraliakbari et al, 2009) we put a programmable camera on a gyrocopter and recorded a first few strips by flying over Stuttgart. The aerial triangulation was successful and a first orthophoto mosaic with 10 cm ground resolution could be derived. In this paper we go a step further and present the experimental setup of our low-cost system together with the first results of gyrocopter image flights using a SLR colour camera and a thermal infrared camera.

We intend to compete with traditional systems and find out the strengths and weaknesses of using small size and low cost systems of aerial photography. In the following sections we discuss the experimental setup of our low-cost system and show first results. Four test flights based on different purposes are described.

Related work

Research has been carried out with regard to investigating the use of low-cost cameras for aerial imaging as well as low-cost GPS/IMU systems for platform orientation. No reports exist about the use of gyrocopters for aerial mapping.
Ahmad (2008) has investigated a camera similar to ours, the Canon EOS D30 SLR. 30 aerial images were taken with this camera in order to make a comparison with large format aerial

photographs. The author emphasizes the need of a careful camera calibration.

Slawomir Grzonka et al. (2009) have used an Xsens MTi – G MEMS IMU for the estimation of attitudes of a flying object - a quad-rotor - in an indoor navigation application. The achieved height accuracy was about 3 cm.

El–Sheimy (2009) has investigated a GPS/IMU MEMS navigation system for direct georeferencing. He pointed out that auxiliary velocity updates can efficiently reduce the position drift during GPS signal outages.

Xiaoji et al. (2006) have investigated utilization of a MEMS-based INS/GNSS integrated system in a direct georeferencing application of mobile mapping. They used real INS/GNSS signals and simulated image measurements. By a mapping simulation it is shown that the accuracy of MEMS can reach some decimeters if satellite signals are available.

Mostafa et. al. (2001) have discussed the direct georeferencing by means of Applanix' POS systems. The authors analyzed the ground accuracy using POS integrated with a digital frame camera. The standard deviation of ground points derived by POS compared to GCP surveyed reference was 0.27 m horizontally and 0.52 m vertically.

Bäumker et. al. (2001) have investigated the misalignment between the body coordinate system established by the IMU and the image coordinate system. The investigation was based on direct georeferencing of 70 aerial images taken by a Kodak DCS 460 CIR camera. First a reference bundle adjustment was carried out to determine coordinates of 500 tie points and use them later on as check points for direct georeferencing. In order to obtain the misalignment parameters, a special calibration was carried out using a travelling crane. The adjustment procedure was based on mathematically rigorous algorithm. After calibration of the misalignments, extremely accurate attitudes of 0.003 gon for ω and φ and 0.011 gon for κ were obtained.

Kremer (2009) has investigated the data acquisition with the IGI DigiTHERM thermal camera system (consisting of one or more thermal cameras) together with the AEROcontrol GNSS/IMU system. He has used an uncooled microbolometer thermal camera. Within this aerial thermal imagery project, an area of 685 km^2 was covered. For direct georeferencing of the thermal images, the radial distortion of the camera and the bore sight misalignment was calculated. A sub block of eight strips containing 50 images in each strip was processed by Match AT INPHO software.

Luiz et al (2008) investigated a technique for object tracking by image sequences. The platform used for taking aerial images was an airship carrying Camera (Point Gray Flea) and IMU. As a result, a 3D map in form of DEM was built.

2. IMAGE FLIGHT AND PROCESSING

As with all projects of aerial photogrammetry a gyrocopter based aerial mapping project has to be planned carefully which includes flight planning, flight navigation, acquiring and processing aerial photographs.

2.1 Planning of the flight

Starting point for flight planning are the spatial extend of the project area, parameters of the available cameras and some output specific parameters, for example, the ground pixel size of the orthoimage which might be the final product of the task. By applying the standards of flight planning parameters like image scale, flying height, side and end lap, etc. are defined. The speed of the gyrocopter can be as slow as 80 km/h. With an exposure time of 1/500 sec or 1/1000 sec only a moderate motion blur effects the images, and the exposure frequency can be relatively low. Another result of flight planning is 3D coordinates of the strip end points which are used by the navigation tool. Due to the maneuverability of the gyrocopter, the reversing track loops can be small.

2.2 Flight navigation

First experiences with navigation tools developed to guide the gyrocopter pilots have shown that a more sophisticated solution is required. That PDAs are used by those guidance tools like GPS Tuner (GPStuner, 2010) is well proven. Therefore one goal of the project is to develop a guidance tool which runs on the PDA. Our current implementation uses a Kalman filter solution which uses the recorded GPS position and velocity data to predict the current flight path. Horizontal and vertical deviations of the predicted state to the planned flight track are determined in real-time and visualized graphically.

2.3 Aerial photography

The conceptual design of our system provides for one or more cameras which are connected to a field computer as shown in Figure 1. In the experimental setup we mounted each camera inside a padded camera box, which on its part is attached on the undercarriage of the gyrocopter. For controlling the cameras a field computer is used which also serves for recording and processing of the GPS/IMU system. The recorded image data are stored on the field computer together with the time tags of image acquisition. Not yet realized is to trigger the cameras with the GPS/IMU sensor. Ahn and Won (2009) discussed the complexity of precise time synchronization and observed a time asynchrony error of 0.1 sec for the PCI delay, 0.3 sec for the UTC time tag error in image files and 0.17 sec for DGPS data delay. With a simple alignment of the camera clock to the GPS time scale we achieved a comparable time synchronization accuracy.

As another challenge of the aerial photography with gyrocopters we expected vibrations of the vehicle. For the TIR camera which not uses the traditional shutter technology for controlling the exposure time blurring due to vibration may appear. An analysis of platform vibrations is given in Section 4.4.2.

2.4 Aerial triangulation, orthophoto and mosaic generation

Aerial triangulation is carried out using GPS/IMU data for the projection centers as prior information together with supporting ground control. Relying on the directly acquired georeference which is available from the low-cost GPS/IMU sensor would not be a proper solution. This first version of our low-cost sensor system uses the aerial triangulation to get around the problem of systematic errors of the system components including the drifts of the IMU. Deviations between the position and attitude data obtained by the GPS/IMU sensor and the exterior orientation parameters determined by the aerial triangulation are discussed in Section 4.4.1.

For orthophoto generation and mosaicking either a DTM or a DSM is used depending on what is available in the project area. In all areas where we carried out our projects so far LiDAR data have been available. By filtering the LiDAR data DTMs as well as DSMs can be created and used for orthorectification of the imagery.

A further issue in this context is the calibration of the overall system (GPS-IMU-cameras) which is not yet analyzed in detail.

3. LOW-COST SENSOR SYSTEM

3.1 Hardware of our current prototype system

The experimental setup of our low-cost system is shown in Figure 1. The basic concept is to integrate airborne sensors, in particular cameras, on a gyrocopter platform together with GPS/IMU and a flight navigation system.

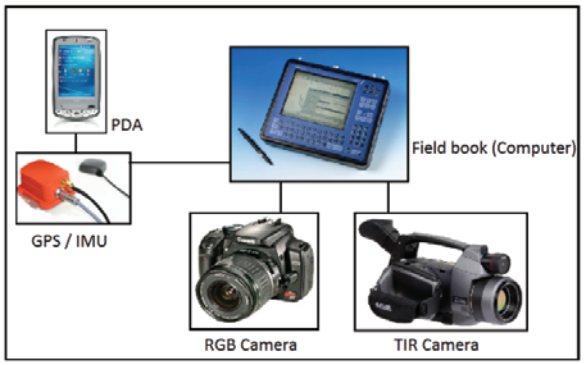

Figure 1. Experimental setup of our low-cost system

Our prototype system consists of the following components:

a) Canon EOS 350D SLR camera
In accordance with the low-cost objective of this project, we selected a common amateur colour camera. The aerial images taken by the Canon camera have a size of 3456 x 2304 pixels which corresponds to a sensor size of 22.2 * 14.8 mm^2 as the pixel size is 6.42 µm. The focal length amounts to 70mm. The field-of-view of the camera is therewith significantly smaller than that one of professional medium and large format aerial cameras; a relatively high exposure frequency is required to provide sufficient overlap of the aerial images.

b) FLIR SC660 thermal infrared camera
SC660 is an uncooled microbolometer TIR camera with a sensor size of 640 x 480 Pixel; pixel size is 25.0 µm. The camera is sensitive for radiation in the wavelength range of 7.5 - 13 µm. According to the producer's specifications, its thermal sensitivity is better than 0.045°C and its temperature range extends from -40°C to 1500°C (FLIR, 2009). The maximum frame rate for these kind of thermal camera is 30 frames per second (FLIR, 2010). Lower price and lighter weight compared to cooled TIR cameras let us favour this camera type.

c) Xsens MTi–G
The integrated GPS and IMU system MTi-G with a navigation and attitude reference system (AHRS) processor (Xsens, 2010) serves for two purposes: first as navigation tool to guide the pilot on the flight according to the flight plan, second, to provide approximate values for the aerial triangulation.

d) Colibri X5 tablet PC
Operation on a flying vehicle demands for a very robust field computer. The thoroughgoing construction of the Colibri tablet PC offers protection from strong vibrations, its monitor provides good contrast also under strong sun illumination.

e) PDA HP iPAQ hx 2790
This pocket PC is used to run the flight guidance software and provide guidance to the pilot. Small size (70 mm * 117.5 mm), light weight (0.165 kg) and proper mounting devices in the gyrocopter cockpit are advantages of the PDA. Using the included GPS, can give the primary position of the gyrocopter.

f) Platform
So far the sensors are installed in boxes, which on their part are attached at the undercarriage of the gyrocopter. For the future we intend to mount the sensors on a special platform together with shock mounts in order to reduce the impact of gyrocopters vibrations.

3.2 Software

For real-time control and post processing of the data recordings, the following software is used:

a) EDSDK2.5 API
EDSDK stands for EOS Digital Camera Software Development Kit. This application programming interface allows the control of the camera from a host PC, in particular the exposure and the download of images to the PC. In this research the EDSDK2.5 is used to control the start, end and frequency of the camera shooting. The exposure interval can be less than 1 second. The images of a strip can be buffered on the memory card and stored on the PC before recoding the images of the next strip.

b) MT Manager
This is a user interface software which simplifies the access to the GPS IMU data. The software enables the monitoring of 3D orientation, inertial and magnetic sensor data as well as positional information in real–time.

c) INPHO's photogrammetric system
Various components of Inpho's photogrammetric system, in particular MatchAT for the aerial triangulation, OrthoMaster for orthophoto generation and OrthoVista for mosaicking are used for the photogrammetric processing of the images.

d) ThermaCAM researcher
The main purpose of this software is the administration of live Thermal IR images arriving through the camera interface (FLIR, 2009). The software controls the frame rate, i.e. the number of images per second to be stored. Stored sequences can be exported as separate frames with appropriate image formats.

e) Software module for flight guidance
A flight path guidance tool is currently being developed (cf. Section 2.2).

4. EXPERIMENTAL INVESTIGATION

Four test image flights have been carried over the city center of Stuttgart and the village Kirchheim unter Teck in Germany.

4.1 Experiment1: A first image flight with the gyrocopter

The aim of the first image flight was to get an early impression on the quality of image recordings taken from a gyrocopter. The flight was carried out at an elevation of 350 meters above the ground with a focal length of 70 mm. With the pixel size of 6.42 µm and an image scale of around 1:5000 this leads to a ground pixel size of 3.2 cm which is a very high resolution for aerial photography.

The area on the ground covered by an image of the EOS 350D SLR camera is significantly smaller than the area covered by professional medium format cameras with the same focal length. Nevertheless the aerial triangulation performed very well with a σ_0 of 6.1 µm which less than one pixel.

Figure 2. Orthophoto mosaic of Kirchheim

Figure 2 shows the generated orthophoto mosaic derived from two strips of this flight using 20 photos.

4.2 Experiment2: RGB image flight over Stuttgart

The second gyrocopter image flight covered four image strips of the city center of Stuttgart. A flying height of 700 meter above ground and a focal length of 70 mm were selected which yields an image scale of 1:10.000. For testing purposes a high end lap of 75% and a side lap of 50% were chosen. The speed of the gyrocopter of 100 km/h leads to a time interval of two seconds between two exposures. Figure 3 shows the flight plan with strips and the actually flown tracks (GPS tracks). The horizontal deviations between the flown and planned tracks are all within 10 m.

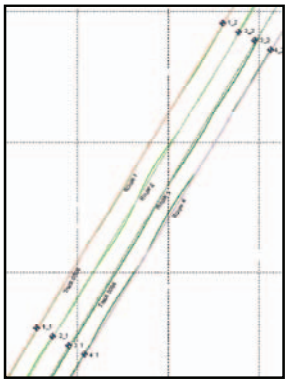

Figure 3. Planned and flown strips

The deviations between planned and the recorded tracks in the vertical direction are up to 50 meter, which reflects the windy day and the current limitations of the flight navigation tool. Visual inspection of the images shows a good overall image quality.
Photogrammetric processing was done as outlined in Section 2.4. A σ_0 of 2.1 µm was achieved by the AT which is close to 1/3 of the camera pixel size thus in this regard a very satisfying result. For orthophoto generation a pixel size of 10 cm was defined. Footprints of the generated orthophotos are shown in Figure 4 a), the resulting orthoimage mosaic in Figure 4 b). The image group adjustment was selected as global tilting in order to avoid radiometric differences between the images (Inpho, 2008)

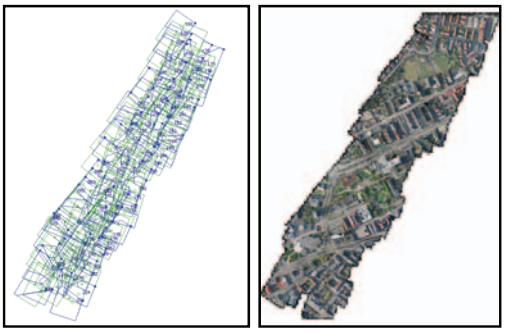

Figure 4 a) Footprint of the orthophotos (left) b) the generated orthomosaic (right)

Figure 5. Some building of the University of Applied Sciences (HFT) Stuttgart

The window of the orthoimage (Figure 5) shows some buildings of the University of Applied Sciences in Stuttgart.
This experiment verifies the potential of our prototype system to deal with aerial survey mapping projects of a certain size.

4.3 Thermal image flight

The thermal image flight aims at recording information about the temperature of the imaged objects for which a camera is used which captures infrared radiation and converts it into a visual image that indicates temperature. There are some requirements for recording the temperature of objects. In particular, the emissivity of the objects must be known. Details on the thermal camera which was used in our image flight experiment are given in Section 3.1.
The TIR image flight covered five image strips. Flight parameters are a 1:5400 photo scale, a focal length of 74 mm and a flying height of 400 m above ground. With a subset of the recorded images (34 TIR images in three strips) aerial triangulation was done and an orthoimage mosaic was created. Even though the TIR images are not as sharp as the RGB images and the size of TIR images is fairly small the photogrammetric processing worked very well. Figure 6 shows the generated orthoimage mosaic.

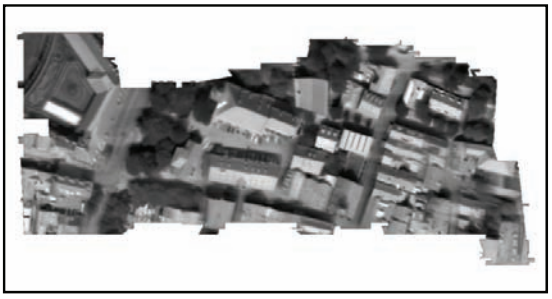

Figure 6. Orthoimage mosaic of thermal aerial images of Kirchheim unter Teck

One possibility to show the potential of the recorded thermal images is to fuse the low resolution thermal orthoimages with high resolution RGB orthoimages (Figure 7). This process is well known as pan-sharpening.

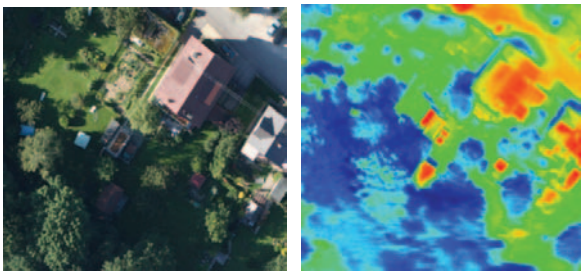

Figure 7. Orthoimages: RGB (left) and TIR (right). The TIR is false colorized. The color scale varies from 20°C (blue) to 57°C (red)

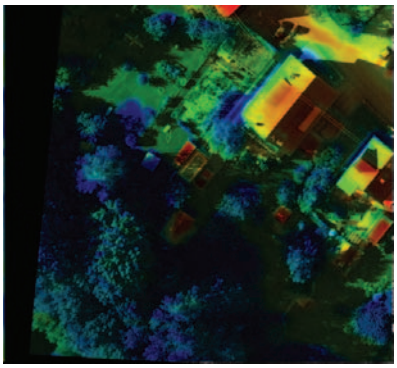

Figure 8. Pan sharpened thermal orthoimage

Figure 8 shows the pan-sharpened thermal orthoimage. The interpretation of this image in terms of relating the temperature information to the objects of interest is fairly easy and provides a good basis for thermographic investigations. Even though the RGB and TIR images have been recorded with a time delay of a few hours (a closer look to the RGB and TIR shadow areas in Figure 8 reveals) the achievements are very encouraging.

4.4 Experiment with GPS/IMU Xsens MTI-G

Two aims are pursuit with the first flight with the GPS/IMU sensor. One is to get a first idea about the potential of the system for platform orientation and second to investigate vibrations of the gyrocopter platform.
Two RGB image strips haven been recorded of Kirchheim unter Teck. Flight parameter specifications have been doen as in the previous experiments (focal length 70 mm, flight elevation 500m above ground, image scale around 1:7000). By photogrammetric processing an orthoimage mosaic with 5 cm ground pixels size was generated which is depicted in Figure 9.

Figure 9. Orthoimage mosaic of 2 strips

4.4.1 Comparison of IMU and aerial triangulation results

The GPS/IMU system employs a Kalman Filter solution (loose coupling) to determine position (X, Y, Z) and attitude (roll, pitch and yaw) at a rate of 120 Hz. Details can be found in XSens (2010). In a first test we focus on the attitude parameters and compare it with the results obtained from the aerial triangulation.
The figures below show the recoded data for the three IMU angles and the three AT angles in one graph as well as the differences between the corresponding angles. Parameterisation of both IMU and AT angles is chosen in a way that they can be directly related to each other.

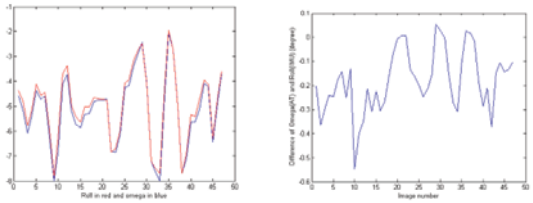

Figure 10. Roll (red) and omega (blue) is shown in the left graph and the difference between both shown in the right one.

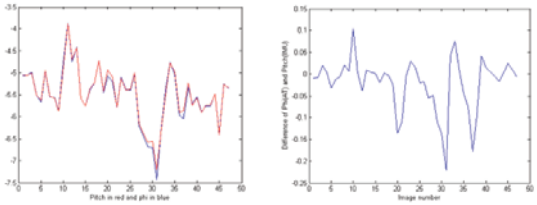

Figure 11. Pitch (red) and phi (blue) is shown in the left graph and the difference between both shown in the right one

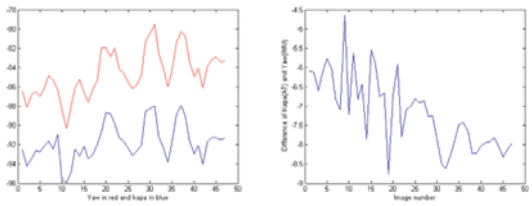

Figure 12. Yaw (red) and kappa (blue) is shown in the left graph and the difference between both shown in the right one

Differences between the results of IMU and the Aerial triangulation are summarised in the following table (Table 1).

	omega-roll	pitch-phi	yaw-kappa
Mean value of differences	-0.1794	-0.0210	-7.1704
Standard deviation of differences	0.1300	0.0609	0.9500

Table 1. Differences between the results of IMU and the AT (units are degree)

The mean values of the differences indicate slight shifts for omega/roll and pitch/yaw and a significant misalignment between yaw and kappa. The standard deviations (mean free) indicate that omega/roll and pitch/yaw coincide at the 1/10 of degree level. The standard deviations with respect to yaw/kappa

will become interpretable after a proper alignment (mainly) in this direction.

4.4.2 Vibration analysis of gyrocopter

The investigation of vibrations of the gyrocopter platform is another crucial aspect for the development of the sensor platform. Apart from the wind-induced oscillations, the vibrations induced by the motor, the propeller and by the main rotor are prominent, see Table 2 for the typical frequencies. The propeller is gear-reduced with a factor of 2.43, therefore the propeller frequency is lower than the motor frequency by this factor. In general the induced vibrational frequencies differ from the excitation frequencies: As the propeller features three blades, its induced vibration frequency is three times higher than the propeller frequency itself. The rotor has two blades which yields a frequency doubling.

Excitation	Typical frequencies(Hz)	Vibrational frequencies (Hz)
Motor	75 - 95	
Propeller	30 – 40	90 – 120
Rotor	5.8 – 6.7	11.6 – 13.4

Table 2. Typical and vibrational frequencies in motor, Propeller and Rotor

During a test flight the oscillations of the accelerations and of the orientation angles have been recorded by an IMU with a sampling rate of 120 Hz. A Discrete Fourier Transform (DFT) of these observed quantities was performed according to eqn (1) for a relatively calm interval of the flight.

$$\hat{\tilde{f}}(n\Delta\nu) = c_n = \frac{1}{N}\sum_{k=0}^{N-1} f(k\Delta t)\exp\left(-i\frac{2\pi}{N}kn\right) \tag{1}$$

Here N denotes the number of observations within the sample, $\Delta\boldsymbol{\nu}$ is the basic frequency of the interval, c_n the Fourier coefficient.
Figures (13) show the square roots of the power spectra of the DFTs for the accelerations and the orientation angles.

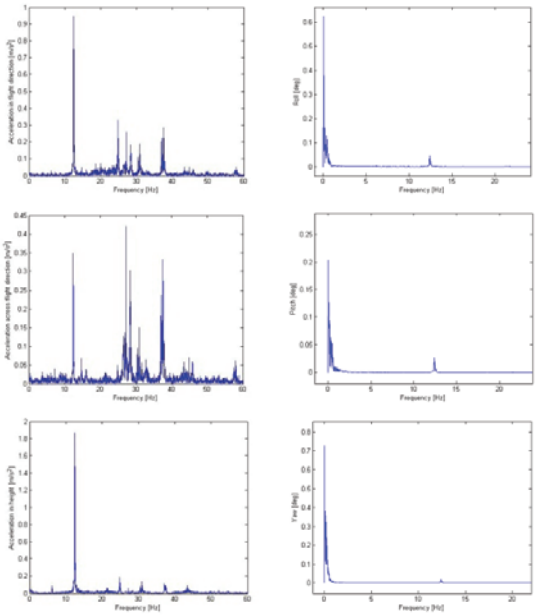

Figure 13. Square root of power spectra of accelerations (left column) and orientation angles roll, pitch, yaw (right column)

Although the sampling interval amounted to considerable 34 s, the Fourier spectra show distinct peaks. For the accelerations along track and in height direction, the rotor-induced term at 12.5 Hz is predominant. In all acceleration plots, additional terms in the range between 20 Hz to 45 Hz are available which, however, mostly do not reach the amplitude of the „rotor term“. It might be guessed that the propeller contributes with a term of its original frequency. On the other hand, also aliasing effects are possible, as the propeller-induced vibration frequency exceeds the Nyquist frequency of 60 Hz. The aliasing can be modelled according to the well-known rule

$$\hat{\tilde{f}}(\nu) = \hat{f}(\nu) + \hat{f}\,(\nu + \nu_s) + \hat{f}\,(\nu - \nu_s) \tag{2}$$

Here $\boldsymbol{\nu}_S$ denotes the sampling frequency. $\hat{f}(\nu)$ is the spectrum of the actual signal and $\hat{\tilde{f}}(\nu)$ the aliased spectrum. Let $\boldsymbol{\nu}_A$ be the frequency of the high-frequent aliasing signal. The contaminated frequencies are therefore

$$\nu = \nu_A - \nu_S \tag{3}$$

In our case $\boldsymbol{\nu}_A$ varies in the range of 90-120 Hz. We may therefore expect that the frequencies between 0 and 30 Hz are contaminated.

The spectra of the orientation angles also show an obviously rotor-induced peak. Apart from this, there are significant amplitudes only for very low frequencies, which might be excited by the wind and by steering actions of the pilot. Also here aliasing effects on the low-frequent angular oscillations cannot be excluded. In view of the concentration of the observed spectra around the zero frequency, they seem to be very improbable, however. Accepting this assumption, the low-frequent oscillations seem to be negligible. As the integration time of the thermal camera is typically about 5 ms, oscillations with frequencies below 1 Hz are hardly affecting the data quality of the recorded images.

In general, angular oscillations are much more critical for the data quality than translational vibrations. The maximal perturbation al velocities during the test interval are in the order of 1 m/s. This is far below the flight velocity of about 30 m/s and causes an additional motion blur of less than 1cm at ground, if an exposure time of 5 ms is assumed. On the other hand, temporal derivatives of pitch and roll of 0.2 rad/s and 0.3 rad/s were encountered. Within the integration time of 5 ms this causes a change in pitch and roll of 1 mrad or 1.5 mrad, respectively. For a flying height of 400m, this corresponds to a ground displacement of more than 40 cm or 60 cm, respectively. For ground resolution of 10 cm, this means a blurring of three or four pixels at least.

5. CONCLUSION AND FURTHER WORK

Due to its low acquisition prize and low fuel consumption, the gyrocopter is a very economic platform for image flights. The main purpose of this research is to develop a low-cost prototype system for aerial survey and show that a photogrammetric product like an orthophoto with a 10 cm ground resolution can be acquired and generated with low-cost equipment mounted on a gyrocopter. First steps of the technical implementation of our prototype system have been successfully completed and the four test flights show that we have derived promising RGB

orthophotos and mosaics as shown in this paper. No errors have been observed along seamlines which indicates that the geometric quality our images can compete with professional standard. Visual inspection furthermore shows that colors and sharpness of the generated orthoimage mosaic are equivalent to standard orthoimages. In addition, we have successfully performed the same processing with TIR imagery.

By means of the recorded IMU observations, we have analyzed the vibrational oscillations of the flying platform in position and attitude. We identified a rotor-induced vibration of about 13 Hz as the most important perturbation source of the gyrocopter affecting the image quality.

For a future improvement of the system, we plan to establish a better time synchronization procedure between camera and GPS/IMU. In particular for the TIR camera, a careful calibration should reduce the lens distortion. The sensors are to be installed on a common shock-mount platform in order to reduce the vibrations. The flight path guidance tool must be improved to enable the pilot to keep the projected track more precisely. Such a tool is currently implemented on the existing PDA. The drift of the accelerometers and the gyros of the IMU should be more closely investigated.

6. REFERENCES

Ahmad, A., 2008. Digital Photogrammetry: An Experience of Processing Aerial Photograph of UTM acquired using digital camera. http://eprints.utm.my/490/1/Anuar_Ahmad_fksg.pdf (accessed 15 April. 2010)

Ahn, H.-S. and Won, C.-H., 2009. DGPS/IMU integration-based geolocation system: Airborne experimental test results, Aerospace Science and Technology 13, p. 316–324.

El–Sheimy, N., 2009. Emerging MEMS IMU and its impact on mapping applications, Calgary Canada, Photogrammetric week Stuttgart Germany 2009

FLIR, FLIR SC660 http://www.flir.com/uploadedFiles/Thermography_APAC/Products/Product_Literture/SC660_Datasheet%20APAC.pdf (accessed 10 April. 2010)

FLIR, 2010. FLIR SC600 Series http://www.flir.com/thermography/APAC/en/content/?id=14000, (accessed 10 April. 2010)

Bäumker, M. and Heimes, F.J., 2001.New Calibration and Computing Method for Direct Georeferencing of Image and Scanner Data Using the Position and Angular Data of an Hybrid Inertial Navigation System, FH Bochum University of Applied Sciences

Grzonka, S., Grisetti, G. and Burgard, W., 2009. Towards a Navigation System for Autonomous Indoor Flying, http://www.slawomir.de/publications/grzonka09icra/grzonka09icra.pdf, (accessed 10 April. 2010)

GPStuner, 2010. GPS Tuner Essentials - Get what you need. http://www.gpstuner.com/ (accessed 10 April. 2010)

Kremer, J., 2009. Optimized data acquisition with the IGI DigiTHERM Thermal Camera System, Photogrammetric week Stuttgart Germany

Luiz G., Mirisola, B. and Dias, J.,2008. Tracking from a Moving Camera with Attitude Estimates, ISR-Institute of Systems and Robotics University of Coimbra, Portugal

Miraliakbari, A. , Hahn, M. and Engels, J. ,2009. Aerial survey with a gyrocopter, Applied Geoinformatics for Society and Environment, Stuttgart Germany

Mostafa,M. and Hutton J., Direct positioning and orientation systems. How do they work? What is the attainable accuracy? APPLANIX Corporation, 85 Leek Cr., Richmond Hill Ontario, Canada L4B 3B3

Reference manual,2008, OrthoVista, Inpho GmbH.

User Manual, 2009, ThermaCAM Researcher, FLIR.

User Manual, 2009, MT manager, Xsens.

User Manual technical documentation, 2009, MTi- G, Xsens.

Xiaoji NIU, Hassan, T., Ellum, C. and El-Sheimy, N.,2006. Directly Georeferencing Terrestrial Imagery using MEMS-based INS/GNSS Integrated Systems, XXIII FIG Congress. Munich, Germany, October 8-13.

7. ACKNOWLEDGEMENT

The authors thank Pascal Bouygues (Flugschule Gyrocopter Stuttgart-München) and Roland Geipert(FLIR SYSTEMS) for their support throughout the project.